

# The Effect of Plasmonic Nanoparticles on the Optoelectronic Characteristics of CdTe Nanowires

Lin-Bao Luo,\* Xiao-Li Huang, Ming-Zheng Wang, Chao Xie, Chun-Yan Wu, Ji-Gang Hu, Li Wang, and Jian-An Huang\*

*In this work, a simple strategy is proposed to improve the device performance of photodetector by modifying plasmonic nanoparticles onto the surface of semiconductors nanostructure. Both experimental analysis and theoretical simulation show that the plasmonic metal nanoparticles (AuNPs) exhibits obvious localized surface plasmon resonance (LSPR) which can trap incident light efficiently, leading to enhanced photocurrents and improved performance of photoelectronic devices. It is also observed that the AuNPs modified CdTeNW photodetector exhibit apparent sensitivity to 510 nm light, to which pure CdTeNWs is virtually blind. What is more, after AuNPs decoration, the response speed of the photodetector is increased substantially from 6.12 to 1.92 s. It is believed that this result will open up new doors for manipulating light and further improving the efficiency of semiconductor nanostructures based optoelectronic devices.*

## 1. Introduction

Noble metals, especially gold and silver nanoparticles exhibit unique and tunable optical properties on account of surface plasmon resonance (SPR) which is the collective oscillation of electrons in a solid stimulated by incident light.<sup>[1]</sup> Extensive study have revealed that the frequency and intensity of surface plasmon absorption bands were sensitive to the

type of materials and the morphology, distribution, as well as to the surrounding media. By this token, SPR is able to provide a label-free means of observing binding interactions between an injected analyte and an immobilized biomolecules in real time. To date, a great deal of work dealing with the theories and applications of SPR has been widely investigated.<sup>[2–4]</sup> For example, in 1982 Nylander and Liedberg demonstrated the use of SPR for gas detection and biosensing applications.<sup>[5,6]</sup> Since then SPR, as a surface oriented method, has shown a great potential for affinity biosensors, allowing real-time analysis of biospecific interactions without the use of labeled molecules. In addition to these sensing applications, SPR has also found application in various optoelectronic devices including solar cells,<sup>[7–9]</sup> optical waveguide,<sup>[10,11]</sup> plasmonic nanoantenna,<sup>[12,13]</sup> electrochromic devices,<sup>[14]</sup> photodetectors,<sup>[2,15,16]</sup> and light emitting diodes (LEDs).<sup>[17–19]</sup>

Cadmium telluride (CdTe), as a typical semiconductor material of II–VI group, has garnered increasing research interest lately due to the unique electrical and optical properties. The appropriate band-gap of CdTe ( $E_g = 1.5$  eV at room temperature) and the high optical absorption coefficient in the visible spectrum ( $>10^4$  cm<sup>-1</sup> in the red, approaching

Prof. L.-B. Luo, X.-L. Huang, M.-Z. Wang,  
C. Xie, Dr. C.-Y. Wu, Dr. J.-G. Hu, Dr. L. Wang  
School of Electronic Science and  
Applied Physics and Anhui Provincial Key Laboratory  
of Advanced Functional Materials and Devices  
Hefei University of Technology  
Hefei, Anhui 230009, P. R. China  
E-mail: luolb@hfut.edu.cn

Dr. J.-A. Huang  
Center of Super-Diamond and Advanced Films (COSDAF)  
and Department of Physics and Materials Science  
City University of Hong Kong  
Hong Kong, SAR, P. R. China  
E-mail: vjahuang2-c@my.cityu.edu.hk



DOI: 10.1002/sml.201303388

$10^5 \text{ cm}^{-1}$  in the blue) allow efficient absorption of sun light, which renders CdTe one of the most promising materials for photovoltaic applications.<sup>[20,21]</sup> Besides, CdTe can act as visible light photodetector as well.<sup>[22]</sup> Dai *et al.* demonstrated that single-crystalline CdTe nanowires from chemical vapor deposition method exhibited obvious photoresponse to 633 nm light illumination, with high photocurrent decay ratio, high responsivity and fast response time.<sup>[23]</sup> What is more, it is also reported that CdTe nanoribbons converted from ZnTe nanobelts were ultra-sensitive to visible-NIR illumination with high gain and responsivity.<sup>[24]</sup> In spite of these progresses, however, the performance of CdTeNW-based photodetectors reported to date is still limited by the low photoresponsivity and very low external quantum efficiency largely due to the extremely small absorption cross-section of the CdTeNWs. A possible technique to increase the light absorption is to functionalize the nanostructures with plasmonic nanoparticles. It is found that by properly engineering the semiconductor/metal structure, the incident light can be efficiently concentrated into semiconductor. These optical phenomena, normally known as localized surface plasmons resonance (LSPRs) and surface plasmon polaritons propagating have been widely used in thin film photovoltaic devices.<sup>[25,26]</sup> Herein, we present a study on improving the device performance of photodetector by modifying plasmonic nanostructures onto the surface of CdTeNW. The plasmonic metal nanoparticles (AuNPs) can induce LSPR which can trap incident light efficiently, leading to enhanced photocurrents and improved performance of photoelectronic devices. In addition, the AuNPs modified CdTeNW photodetector exhibit apparent sensitivity to 510 nm light, to which pure CdTeNWs is virtually blind. We believe this study would open up new opportunities to optimize the device performance of semiconductor nanostructures based photodetectors.

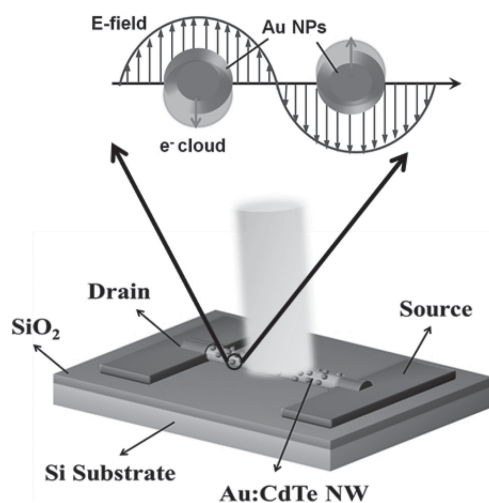


**Figure 1.** Schematic illustration of the AuNPs decorated CdTeNW photodetector, the inset shows the schematic of plasmon oscillation of AuNPs.

## 2. Results and Discussion

**Figure 1** illustrates the proof-of-concept device which is composed of a straight CdTe NW decorated with numerous plasmonic gold nanoparticles. The SEM image of the as-synthesized CdTeNWs is shown in SI-Figure 1. It can be seen that the CdTeNWs have smooth surface and uniform diameter along the growth direction. The NWs are about several hundred microns in length and 200–600 nm in width. The TEM image in **Figure 2(a)** indicates that the CdTeNWs are of single crystalline. The energy dispersive spectrometer (EDS) analysis in the inset confirms that the CdTeNWs consist of only Cd and Te with an atomic ratio of about 1:1. From the high-resolution transmission electron microscopy (HRTEM) image and the corresponding selected-area electron diffraction (SAED) pattern in **Figure 2(b)**, we can find that the intrinsic CdTeNWs are hexagonal zinc blende structure growing along  $[2\bar{1}1]$  orientation with lattice spacing of 0.38 nm. **Figures 2(c)** and **(d)** show the TEM and HRTEM images of Au nanoparticles decorated CdTeNWs, respectively. Due to the distinct difference in contrast, the gold nanoparticles are easily distinguished from the CdTeNW (**Figure 2(c)**). The corresponding lattice resolved image from HRTEM (**Figure 2(e-f)**) reveals a *d*-spacing value of 0.23 and 0.38 nm, in accordance with the *c* lattice constant of Au and CdTe, respectively. The presence of Au nanoparticles was also confirmed by the X-ray photoelectron spectroscopy (see SI-Figure 2). Examination of more nanowires concludes that the majority of the AuNPs are spherical in morphology, with diameters in the range of 10 to 60 nm (Please refer to the statistic distribution shown in SI-Figure 3).

Electrical analysis in **Figure 3(a)** reveals that the single pure CdTe nanowire based FET exhibits typical *p*-type conduction behavior. That is, the electrical conduction decreases with increasing gate voltage. The inset of **Figure 3(a)** plots a representative transfer curve at  $V_{DS} = 5 \text{ V}$  from the same device. By fitting the linear part of  $I_{DS}-V_G$  curve and assuming a cylinder on an infinite plate model for the device, the hole mobility ( $\mu_h$ ), and transconductance ( $g_m$ ) are calculated to be  $0.22 \text{ cm}^2\text{V}^{-1}\text{s}^{-1}$ , and  $0.45 \text{ nS}$  (please refer to the supporting information for detailed calculation), respectively, which are comparable with literature value.<sup>[27]</sup> Interestingly, once Au nanoparticles were decorated onto the NW surface, both hole mobility and transconductance are found to increase by 2 orders of magnitude, to  $41.65 \text{ cm}^2\text{V}^{-1}\text{s}^{-1}$ , and  $85.2 \text{ nS}$ , respectively (**Table 1**). In addition, the holes concentration decreases considerably from  $1.5 \times 10^{15}$  to  $4.5 \times 10^{14} \text{ cm}^{-3}$ . These changes in electrical properties can be probably ascribed to the spontaneous transfer of free carriers between the metal nanoparticles and the NWs, as a result of difference in work functions.<sup>[28]</sup>

To unveil the effect of plasmonic AuNPs on the optoelectronic characteristics of CdTe nanowire. We compared the device performance of CdTeNW based photodetector with and without surface modification. **Figure 4(a)** depicts the typical *I*-*V* curves of a single pure CdTeNW, measured in

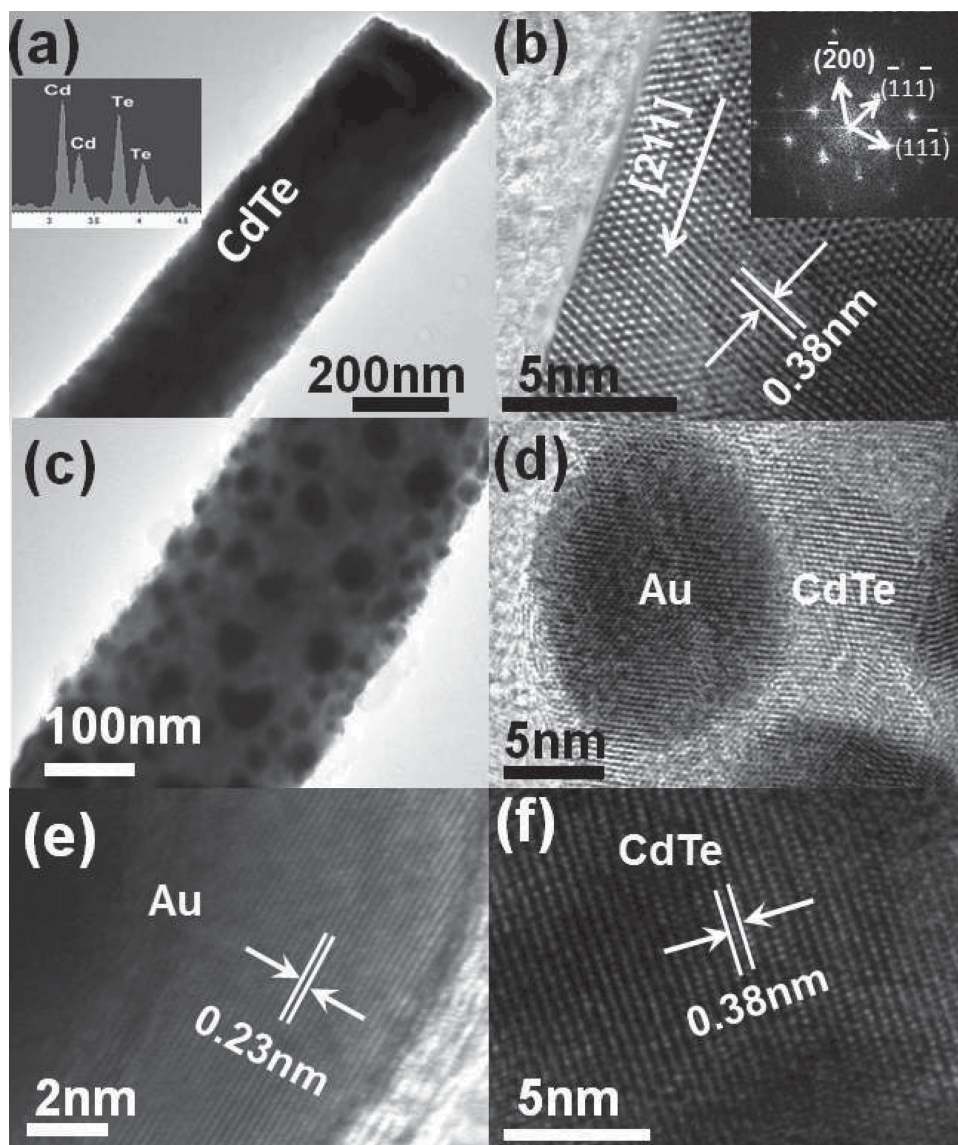


**Figure 2.** (a) TEM image of a typical pure CdTeNW, the inset shows the corresponding EDS spectrum. (b) HRTEM image of a pure CdTeNW, the inset shows the corresponding FFT pattern. (c) TEM image of an AuNPs decorated CdTeNW. (d) HRTEM image of the AuNPs decorated CdTeNW. (e) and (f) HRTEM images of the AuNPs and CdTeNW, respectively.

the dark and under 800 nm light illumination ( $100 \mu\text{Wcm}^{-2}$ ), respectively. Obviously, one can see that the current is only 0.5 nA in dark condition, but increases by four times to 2.1 nA when shined by 800 nm light illumination. Such an increase in current is understandably due to the generation of electron-hole pairs in the NW by photons with energy large than the band gap of CdTe (1.5 eV).<sup>[29]</sup> Notably, the increase in current is much higher for CdTeNW photodetector decorated with plasmonic Au nanoparticles. As shown in Figure 4(b), the current of AuNPs:CdTeNW is less than 4 nA in dark. Upon illuminated with 800 nm light (intensity:  $0.01 \text{ mWcm}^{-2}$ ), the current is observed to increase dramatically by more than 25 times to 100 nA. Figure 4(c) plots the dark current and photocurrent of 6 representative devices, with lines indicating the  $I_{\text{dark}}$  (without AuNPs),  $I_{\text{light}}$  (without AuNPs),  $I_{\text{dark}}$  (with AuNPs) and  $I_{\text{light}}$  (with

AuNPs) of 0.41, 2.2, 3.5, and 109.6 nA, respectively. The relatively high conductance of CdTeNW in dark after decoration of AuNPs can be probably attributed to the transfer of free carriers between the metal nanoparticles and the NWs. As matter of fact, similar phenomenon has been observed on r thin film materials as well.<sup>[30]</sup> What is more, the high photocurrent of AuNPs@CdTeNW over pure CdTeNW is, according to the theoretical simulation based on FDTD, due to the strong LSPR of the AuNPs.

In order to evaluate the effect of gold nanoparticles on the photoconductive property in a quantitative way. The responsivity ( $R$ ), one of the key metrics for a photodetector is calculated by the following formula:<sup>[31]</sup>

$$R (\text{A W}^{-1}) = \left( \frac{I_p}{P_{\text{opt}}} \right) = \eta \left( \frac{q\lambda}{hc} \right) G \quad (1)$$

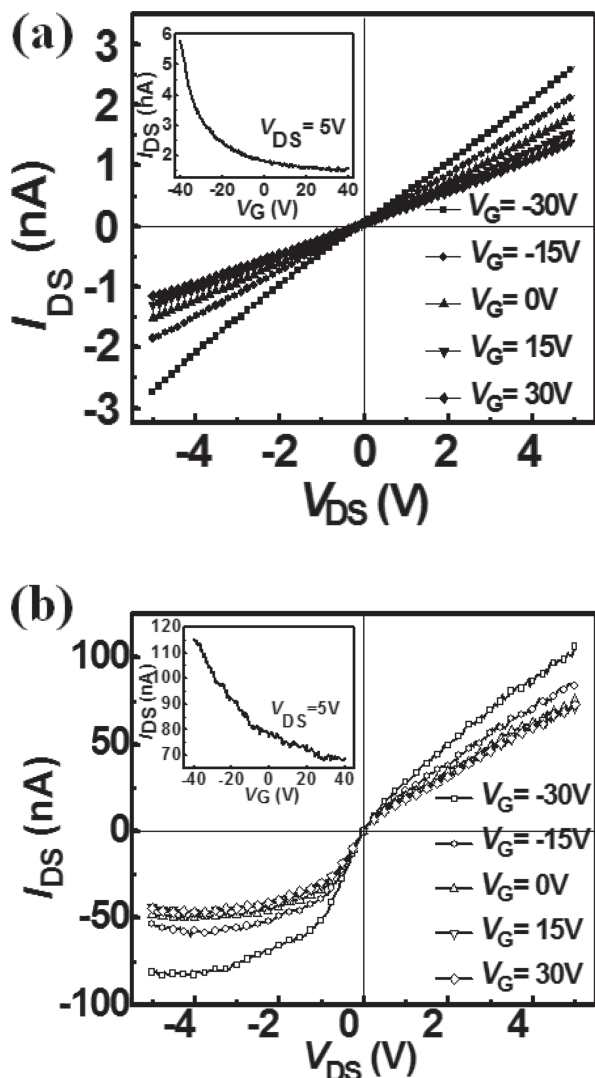


**Figure 3.** (a)  $I_{DS}$ - $V_{DS}$  curves of the pure CdTeNW, the inset shows the  $I_{DS}$ - $V_G$  curve. (b)  $I_{DS}$ - $V_{DS}$  curves of AuNPs@CdTeNW, the inset shows the  $I_{DS}$ - $V_G$  curve.

where  $I_p$ ,  $P_{opt}$ ,  $\eta$ ,  $\lambda$ ,  $h$ ,  $c$  and  $G$  are the photocurrent, the incident light power, the quantum efficiency, the light wavelength, the Planck's constant and the photoconductive gain, respectively. By assuming  $\eta = 1$  for simplification,  $R$  is estimated to be  $3.6 \times 10^2$  and  $2.26 \times 10^4$   $AW^{-1}$  for pure CdTeNW and AuNPs:CdTeNW, respectively. What is more,  $G$  is calculated to be  $5.56 \times 10^2$  for pure CdTeNW, and  $3.5 \times 10^4$  for AuNPs:CdTeNW. In addition, the specific detectivity ( $D^*$ ), a figure of merit normally used to characterize

performance, is calculated as well. This parameter can be expressed as:<sup>[32,33]</sup>

$$D^* = \frac{1}{NEP} \approx \sqrt{\frac{A}{2eI_d}} R \quad (2)$$

Where  $A$  is the PD area,  $q$  the elementary charge of an electron,  $I_d$  the dark current. Based on the equation,  $D^*$  is estimated to be  $6.63 \times 10^{10}$   $cmHz^{1/2}W^{-1}$  for pure CdTe nanowire, and  $1.25 \times 10^{12}$   $cmHz^{1/2}W^{-1}$  for CdTeNW decorated with AuNPs. **Table 2** summarizes the key metrics of the present device and other CdTe nanostructure based photodetectors. It is visible that after surface modification, both  $G$  and  $R$  are higher than other CdTe nanostructures based photodetectors, including CdTe nanoribbons,<sup>[24,34]</sup> CdTe quantum dots,<sup>[35]</sup> and high-crystallinity CdTeNWs.<sup>[36]</sup> We ascribe the improved device performance to the following two factors: (a) Photonic enhancement. The scattering properties of the large metal nanoparticles can increase the optical path length inside the semiconductor to effectively trap light. As a result, the light absorption in the semiconductor is increased.<sup>[37]</sup> On the other hand, the light absorption can be increased by attaching small metal nanoparticles on the semiconductor, which localize the incident field. The concentrated electromagnetic (EM) field of the plasmon increases the absorption cross section of the semiconductor nanoparticle and enhances the carrier creation rate.<sup>[38]</sup> (b) Transfer of the plasmonic energy from the metal to the semiconductor by direct electron transfer (DET).<sup>[39,40]</sup> Just like a dye sensitizer, the metallic plasmonic nanoparticles (AuNPs) absorb resonant photons and transfer the energetic electron formed in the process of LSPR excitation to the neighboring semiconductors. In other words, this process can directly create electron-hole pairs in the semiconductor, independent of the semiconductor's light absorption characteristics.

To understand the surface plasmon resonance enhanced photodetection, we adopted the Finite-Difference Time-Domain (FDTD) method to simulate the optical properties of a 300 nm CdTeNW modified with spherical AuNPs with diameter in the range of 10–60 nm (SI-Figure 4). **Figure 5(a)** shows both theoretical reflectance and transmittance spectra of the nanostructure. By using the formula of  $A = 1 - T - R$  ( $A$ ,  $T$ , and  $R$  denote absorption, transmittance and reflectance, respectively), we can get the theoretical absorption spectrum which is composed of two strong peaks centered at 545 and 790 nm. The 790 nm peak apparently corresponds to band-gap absorption, and the 545 nm band should include the contribution of AuNPs LSPR peak at 500 nm, as well as the 550 nm peak due to morphology-dependent resonance (MDR) of CdTeNWs.<sup>[41]</sup> This simulation result is in rough agreement with the experimental analysis. **Figure 5(c)** plots the UV-vis absorption spectra of both CdTeNWs and AuNPs modified CdTeNWs. Apparently, the absorption of AuNPs@CdTeNWs is composed of two peaks at 490 and 820 nm, while the pure CdTeNWs have only one strong peak 820 nm. The 820 nm peak in

**Table 1.** Summary of the key device parameters of the FETs based on CdTeNWs.

Materials	$\sigma/Scm^{-1}$	$g_m/nS$	$\mu_h/cm^2V^{-1}s^{-1}$	$n_h/cm^{-3}$	$I_{on}/I_{off}$
CdTe NW	$5.3 \times 10^{-5}$	0.45	0.22	$1.5 \times 10^{15}$	2.1
AuNPs@CdTeNW	$2.9 \times 10^{-3}$	85.2	41.65	$4.5 \times 10^{14}$	24

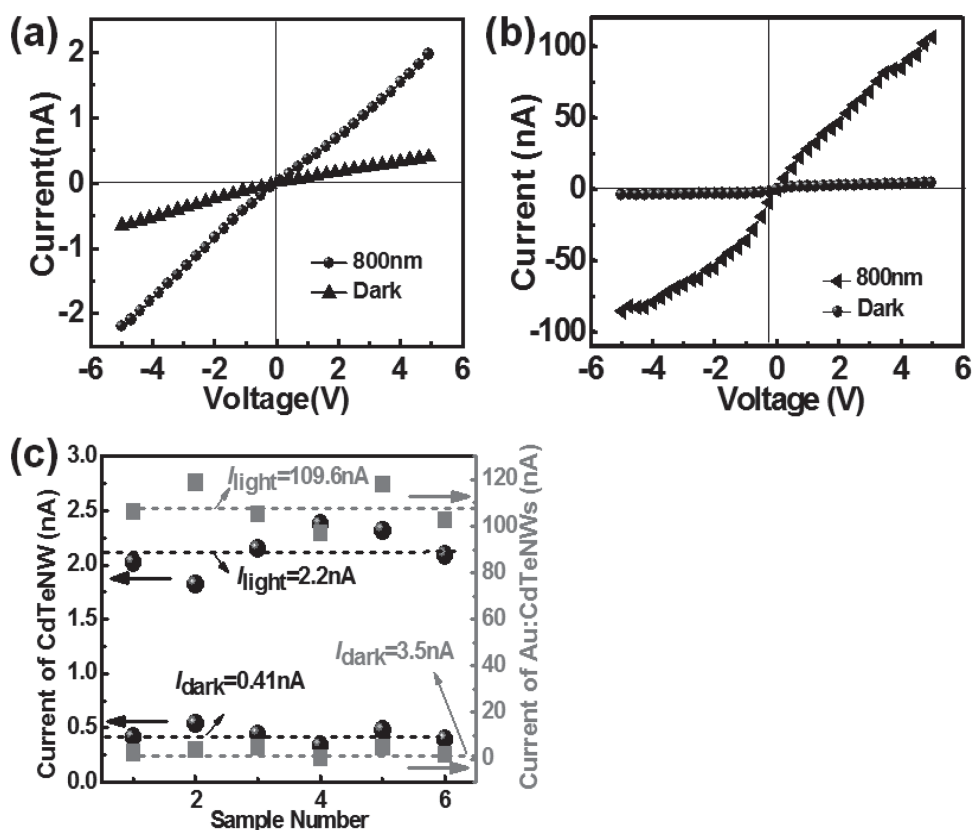


**Figure 4.** (a)  $I$ - $V$  curves of an individual CdTeNW in the dark and under 800 nm-light illumination ( $100 \mu\text{Wcm}^{-2}$ ). (b)  $I$ - $V$  curves of a CdTeNW decorated with AuNPs in the dark and under 800 nm light illumination ( $0.01 \text{ mWcm}^{-2}$ ). (c) The dark current and photocurrent of both 6 representative CdTeNW with and without AuNPs modification.

both absorption curves belongs to the band-gap absorption of CdTeNW. By comparison, the extra peak at 490 nm in the absorption of AuNPs@CdTeNWs is formed after the modification of AuNPs. This phenomenon, known as the localized surface plasmon resonance, is responsible for 490 nm peak in the absorbance curve, and the peak at 510 nm in the spectral response of AuNPs@CdTeNW.<sup>[42,43]</sup> Considering the fact that the LSPR is largely determined by the diameter of the plasmonic metals,<sup>[44]</sup> we believe the broadening of this surface plasmon resonance band is associated with the wide distribution of the diameter of gold nanoparticles.<sup>[45]</sup>

**Table 2.** Summary of device performance of similar semiconductors nanostructures based photodetectors.

Materials	$R/AW^{-1}$	$G$	$D^*/\text{cmHz}^{1/2}\text{W}^{-1}$	Ref.
CdTe NW	$3.6 \times 10^2$	$5.56 \times 10^2$	$6.63 \times 10^{10}$	our work
AuNPs:CdTeTW	$2.26 \times 10^4$	$3.51 \times 10^4$	$1.25 \times 10^{12}$	our work
CdTe NR	—	12.2	—	[34]
CdTe NR	$7.8 \times 10^2$	$2.4 \times 10^3$	—	[35]
CdTe QDs	0.18	—	—	[36]
CdTe NW	19.2	—	—	[37]

We believe the LSPR of AuNPs is responsible for the peak at 490 nm in the experimental absorbance curve of AuNPs@CdTeNWs. To unveil the LSPR effect of AuNPs in a more visible way, we adopted the FDTD method to simulate near-field electric field intensity distributions of AuNPs under light irradiation with wavelengths of 480, 510 and 820 nm (**Figure 6**). Clearly, one can see that 50-nm and 60-nm AuNPs can induce 4- to 8-fold enhancement in dipolar electric energy, while 10-nm AuNPs can only induce less than 2-fold enhancement in energy. This phenomenon is understandable considering the fact that the absorption cross-section of nanoparticle is proportional to the particle volume.<sup>[43]</sup> Further UV-Vis absorption measurements of AuNPs in SI-Figure 5 confirmed that the normalized absorption intensity for 65 and 54 nm AuNPs is much higher than that of 12 nm AuNPs. In light of this, it can be concluded that the plasmon band is mainly due to AuNPs with diameters of both 50 and 60 nm.

It is found that the LSPR can influence the spectral selectivity of the photodetector. **Figure 7(a)** displays the spectral response of both pure CdTeNW and AuNPs decorated CdTeNW based photodetector. Apparently, the photodetector made of AuNPs@CdTeNW was sensitive to incident light at wavelength of 510 nm, to which pure CdTeNW based photodetector is virtually blind. It is worth mentioning that, in addition to increasing the photocurrent and widening

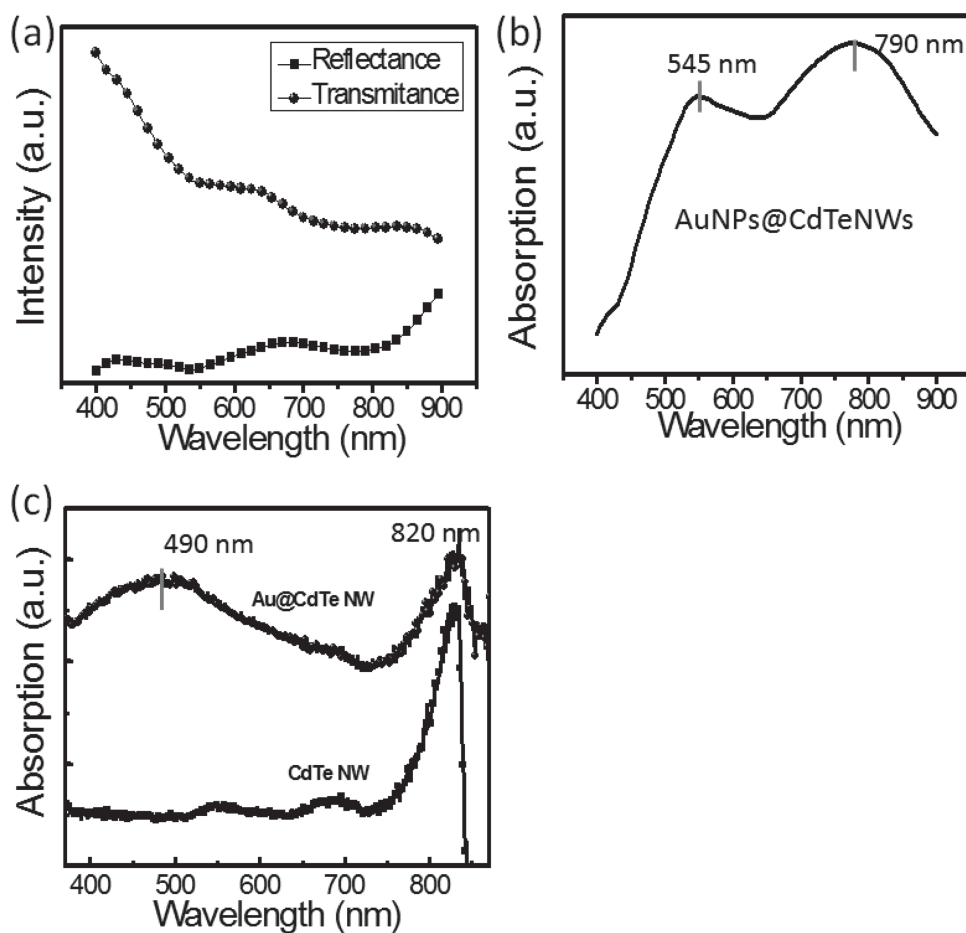


**Figure 5.** (a) Theoretical simulation of both reflectance and transmittance of the AuNPs modified CdTeNWs. (b) Theoretical simulation of the absorption spectrum of the AuNPs modified CdTeNWs. (c) The absorption spectra collected from both CdTeNWs and AuNPs modified CdTeNWs.

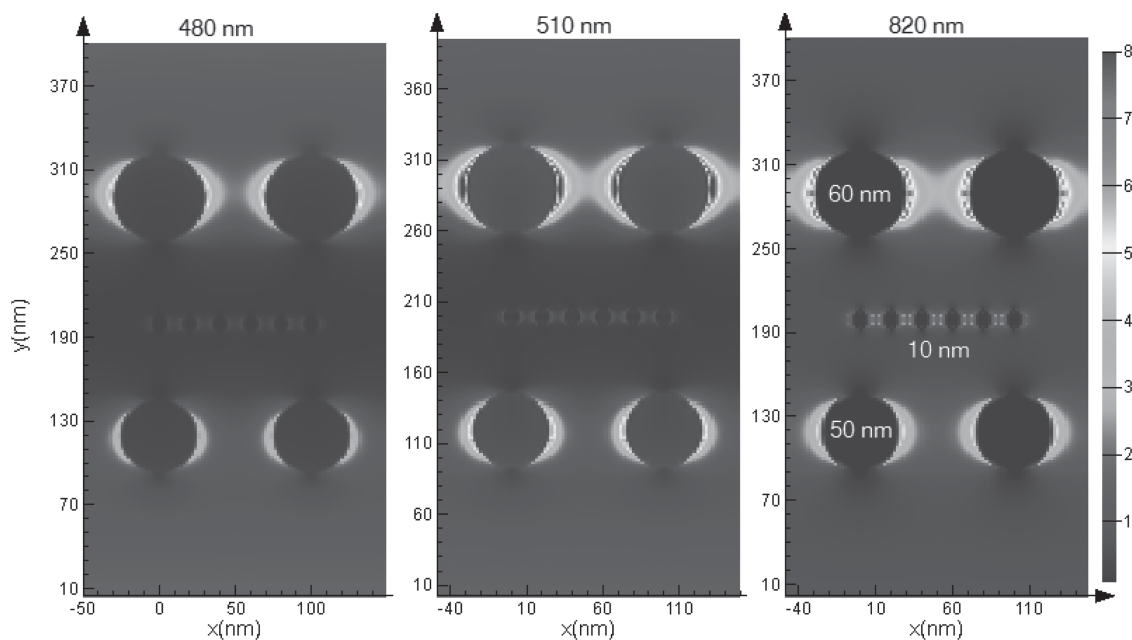


**Figure 6.** Simulated electric field energy density distribution of CdTeNWs decorated with six 10 nm AuNPs, two 50 nm AuNPs, and two 60 nm AuNPs at wavelengths of 480 nm, 510 nm, and 820 nm, respectively.

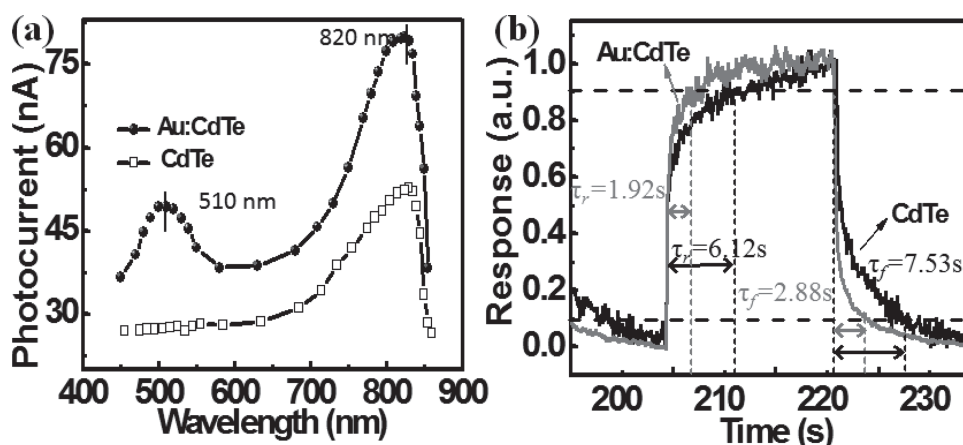


**Figure 7.** (a) Spectral response of both pure CdTeNW and AuNPs decorated CdTeNW based photodetector. (b) A single normalized cycle measured at same incident light for estimating both rise time ( $\tau_r$ ) and fall time ( $\tau_f$ ) of pure CdTeNW and AuNPs decorated CdTeNW, the voltage is 5 V.

the response spectrum, the attachment of plasmonic nanoparticles to the surface of nanostructure are beneficial to improving the response speed as well. Figure 7(b) exhibits the photoresponse of both pure CdTeNW and AuNPs decorated CdTeNWs. In the time domain, the response speed of the IR photodetector is usually assessed by the rise time ( $\tau_r$ ), which is the time interval for the response to rise from 10 to 90% of its peak value. The fall time ( $\tau_f$ ) is the time interval for the response to decay from 90 to 10% of its peak value. By following this definition, the rise and fall time are derived to be 6.12/7.53 s for pure CdTeNW, and 1.92/2.88 s for AuNPs@CdTeNW, respectively. The reason for this phenomenon is yet unclear and need further investigation.

### 3. Conclusion

In conclusion, we systematically explored the influence of plasmonic metal nanoparticles on the optoelectronic characteristics of CdTeNWs. Electrical analysis reveals that after decoration with AuNPs on the CdTeNWs surface, the photocurrent is observed to increase considerably, giving rise to obvious increase in responsivity, detectivity. This enhancement in device performance, according to our theoretical simulation based on FDTD method, is due to the excellent optical property as a result of SPR. It is also found that the response speed was increased by nearly two times after AuNPs decoration. The totality of this study will open up new opportunities for manipulating light and further improving the efficiency of semiconductor nanostructures based photodetectors.

### 4. Experimental Section

**Synthesis and Characterization of Gold Nanoparticles Decorated CdTe Nanowires:** The CdTe nanowires were synthesized by thermal evaporation of pure CdTe powder at 650 °C in a horizontal tube furnace *via* a conventional vapor-liquid-solid (VLS) progress. Au-coated silicon substrates were placed at the downstream position about 10 cm away from the CdTe source material. Before heating,

the system was evacuated to a base pressure of  $10^{-3}$  Pa, and then backfilled with a constant Ar and H<sub>2</sub> (5%) gas flow of 30 SCCM to a pressure of ~250 Pa. Afterwards, the CdTe source was heated up to 650 °C at a rate of 20 °C/min and then the temperature was maintained for 1.5 h. After growth, the furnace was naturally cooled down to ambient temperature and the Si substrate containing black and gray product was collected. The gold nanoparticles were deposited by thermal evaporation at the rate of approximately 2 Å/s with a pressure below  $10^{-3}$  Torr, followed by annealing at 350 °C for 50 min with a constant Ar gas. The phase morphologies and crystal structures of both CdTeNWs and CdTeNWs decorated with AuNPs were characterized by X-ray diffraction (XRD, Rigaku D/Max- $\gamma$ B with Cu K $\alpha$  radiation), field-emission scanning electron microscopy (FESEM, SIRION 200 FEG), and high-resolution transmission electron microscopy (HRTEM, JEOL JEM-2010, at 200 kV) equipped with selected area electron diffraction (SAED). The chemical compositions of the as-synthesized CdTeNWs and Au nanoparticles decorated CdTeNWs were analyzed by X-ray photoelectron spectroscopy (XPS, Thermo ESCALAB 250).

**Device Fabrication and Characterization:** In order to compare the electrical property of CdTeNW before and after modifying gold nanoparticles, a single NW based field-effect transistors (FETs) was fabricated. Firstly, the as-synthesized CdTeNWs were dispersed on a SiO<sub>2</sub> (300 nm thick)/Si wafer with a desired density, and then Cu/Au (10 /50 nm) source and drain electrodes were defined by photolithography and an electron-beam evaporation method. Afterwards, the remaining photoresist was removed by a simple lift-off process. Finally, 5 nm thick gold nanoparticles were deposited on the surface of CdTeNWs using the same electron-beam evaporation system. The Si substrate will serve as the global back gate. Before the measurements, a fast-annealing process at 350 °C for 10 min in Ar gas was carried out such that the Au thin film will nucleate into AuNPs. The electrical characteristics and optical characteristics of the devices were conducted at room temperature by using a semiconductor characterization system (Keithley 4200-SCS) and a monochromatic light source system.

**Theoretical Simulation:** The simulation was done by the numerical FDTD Solutions. The model consisted of 10 nm, 50 nm and 60 nm AuNPs coated on an infinite-long CdTe NW of 300 nm in diameter. The optical data of Au were from Palik and that of CdTe was from Sopra S.A. company database. The illumination was

plane wave of wavelength 400–900 nm with polarization parallel to the axis of CdTe NW. The boundary conditions at x, y were periodic and perfect matching layer (PML) at z.

## Supporting Information

Supporting Information is available from the Wiley Online Library or from the author.

## Acknowledgements

This work was supported by the National Natural Science Foundation of China (NSFC, Nos. 21101051, 61106010, 51172151), and the Fundamental Research Funds for the Central Universities (2011HGZJ0004, 2012HGXC0003, 2013HGCH0012).

- [1] G. Mie, *Ann. Phys.* **1908**, *25*, 377.
- [2] C. C. Chang, Y. D. Sharma, Y. S. Kim, J. A. Bur, R. V. Shenoi, S. Krishna, D. Huang, S. Y. Lin, *Nano Lett.* **2010**, *10*, 1704.
- [3] S. A. Maier, M. L. Brongersma, P. G. Kik, *Adv. Mater.* **2001**, *13*, 1501.
- [4] J. Homola, S. S. Yee, G. Gauglitz, *Sens. Actuators* **1999**, *54*, 3.
- [5] B. Liedberg, C. Nylander, T. Lind, *Sens. Actuators* **1982**, *3*, 79.
- [6] B. Liedberg, C. Nylander, I. Lundstrom, *Sens. Actuators* **1983**, *4*, 299.
- [7] V. E. Ferry, J. N. Munday, H. A. Atwater, *Adv. Mater.* **2010**, *22*, 4794.
- [8] K. R. Catchpole, A. Polman, *Opt. Express* **2008**, *16*, 21793.
- [9] Y. M. Liu, H. W. Zhai, F. Guo, N. Huang, W. W. Sun, C. H. Bu, T. Peng, J. K. Yuan, X. Z. Zhao, *Nanoscale* **2012**, *4*, 6863.
- [10] R. F. Oulton, V. J. Sorger, D. A. Genov, D. F. Pile, X. Zhang, *Nat. Photonics* **2010**, *2*, 496.
- [11] X. Gao, J. H. Shi, X. P. Shen, H. F. Ma, W. X. Jiang, L. M. Li, T. J. Cui, *Appl. Phys. Lett.* **2013**, *102*, 151912.
- [12] Z. Y. Fang, L. R. Fan, C. F. Lin, D. Zhang, A. J. Meixner, X. Zhu, *Nano Lett.* **2011**, *11*, 1676.
- [13] J. Dorfmueller, R. Vogelgesang, W. Khunsin, C. Rockstuhl, C. Etrich, K. Kern, *Nano Lett.* **2010**, *10*, 3596.
- [14] Tsuboi, K. Nakamura, N. Kobayashi, *Adv. Mater.* **2013**, *25*, 3197.
- [15] H. R. Stuart, D. G. Hall, *Appl. Phys. Lett.* **1998**, *73*, 3815.
- [16] J. D. Lin, H. Li, H. Zhang, W. Chen, *Appl. Phys. Lett.* **2013**, *102*, 203109.
- [17] P. A. Hobson, S. Wedge, J. A. E. Wasey, I. Sage, W. L. Barnes, *Adv. Mater.* **2002**, *14*, 1393.
- [18] Köck, E. Gornik, M. Hauser, W. Beinstingl, *Appl. Phys. Lett.* **1990**, *57*, 2327.
- [19] K. Okamoto, I. Niki, A. Shvartser, *Nat. Mater.* **2004**, *3*, 601.
- [20] K. Mitchell, A. L. Fahrenbruch, R. H. Bube, *J. Appl. Phys.* **1977**, *48*, 4365.
- [21] J. Britt, C. Ferekides, *Appl. Phys. Lett.* **1993**, *62*, 2851.
- [22] H. Park, G. Yang, S. Chun, D. Kim, J. Kim, *Appl. Phys. Lett.* **2013**, *103*, 051906.
- [23] Y. Ye, L. Dai, T. Sun, L. P. You, R. Zhu, J. Y. Gao, R. M. Peng, D. P. Yu, G. G. Qin, *J. Appl. Phys.* **2010**, *108*, 044301.
- [24] X. Xie, S. Y. Kwok, Z. Z. Lu, Y. K. Liu, Y. L. Cao, L. B. Luo, J. A. Zapien, I. Bello, C. S. Lee, S. T. Lee, W. J. Zhang, *Nanoscale* **2012**, *4*, 2914.
- [25] H. A. Atwater, A. Polman, *Nat. Mater.* **2010**, *9*, 205.
- [26] V. E. Ferry, L. A. Sweatlock, D. Pacifici, H. A. Atwater, *Nano Lett.* **2008**, *8*, 4391.
- [27] L. Zhu, J. S. Jie, D. Wu, L. B. Luo, C. Y. Wu, Z. F. Zhu, Y. Q. Yu, L. Wang, *J. Nanoeng. Nanomanuf.* **2012**, *2*, 191.
- [28] N. Han, F. Y. Wang, J. J. Hou, S. P. Yip, L. Hao, F. Xiu, M. Fang, Z. X. Yang, X. L. Shi, G. F. Dong, T. F. Hung, J. C. Ho, *Adv. Mater.* **2013**, *25*, 4445.
- [29] L. B. Luo, F. X. Liang, J. S. Jie, *Nanotechnology* **2011**, *22*, 485701.
- [30] K. Kim, D. L. Carroll, *Appl. Phys. Lett.* **2005**, *87*, 203113.
- [31] B. Nie, L. B. Luo, J. J. Chen, J. G. Hu, C. Y. Wu, L. Wang, Y. Q. Yu, Z. F. Zhu, J. S. Jie, *Nanotechnology* **2013**, *24*, 095603.
- [32] J. M. Liu, *Photonic devices*, Cambridge University Press, Cambridge, **2005**.
- [33] L. H. Zeng, M. Z. Wang, H. Hu, B. Nie, Y. Q. Yu, C. Y. Wu, L. Wang, J. G. Hu, C. Xie, F. X. Liang, L. B. Luo, *ACS Appl. Mater. Interfaces* **2013**, *5*, 9362.
- [34] M. C. Kum, H. Jung, N. Chartuprayoon, W. Chen, A. Mulchandani, N. V. Myung, *J. Phys. Chem. C* **2012**, *116*, 9202.
- [35] C. C. Tu, L. Y. Lin, *Appl. Phys. Lett.* **2008**, *93*, 163107.
- [36] Y. Ye, L. Dai, T. Sun, L. P. You, R. Zhu, J. Y. Gao, R. M. Peng, D. P. Yu, G. G. Qin, *J. Appl. Phys.* **2010**, *108*, 044301.
- [37] H. A. Atwater, A. Polman, *Nat. Mater.* **2010**, *9*, 205.
- [38] S. Linic, P. Christopher, D. B. Ingram, *Nat. Mater.* **2011**, *10*, 911.
- [39] S. K. Cushing, N. Wu, *Electrochem. Soc. Interface* **2013**, *63*.
- [40] S. Linic, P. Christopher, D. B. Ingram, *Nat. Mater.* **2011**, *10*, 911.
- [41] S. A. Maier, *Plasmonics: fundamentals and applications*, Springer, New York **2007**.
- [42] Z. D. Lu, J. Goebel, J. P. Ge, Y. D. Yin, *J. Mater. Chem.* **2009**, *19*, 4597.
- [43] Q. Zhang, D. Q. Lima, I. Lee, F. Zaera, M. F. Chi, Y. D. Yin, *Angew. Chem. Int. Ed.* **2011**, *123*, 7226.
- [44] Tsuboi, K. Nakamura, N. Kobayashi, *Adv. Mater.* **2013**, *25*, 3197.
- [45] M. L. Brongersma, P. G. Kik, *Surface plasmon nanophotonics*, Springer, Dordrecht, **2007**.

Received: October 30, 2013  
 Revised: February 20, 2014  
 Published online: March 7, 2014